

Theoretical investigations on the structural, spectroscopic, electronic and thermodynamic properties of (3-Oxo-3H-benzo[f]chromen-1-yl) methyl N,N-dimethylcarbamdithioate-1ex

MEHMET KARA¹, MERYEM EVECEN^{2,*}, TELHAT ÖZDOĞAN³

¹Mechanical Engineering, Technology Faculty, Amasya University, 05100 Amasya, Turkey

²Department of Physics, Faculty of Arts and Sciences, Amasya University, 05100 Amasya, Turkey

³Department of Computer and Teaching Technology Education, Education Faculty, Amasya University, 05100 Amasya, Turkey

Hartree-Fock and Density Functional Theory (B3LYP, B3PW91) calculations for the ground state of (3-Oxo-3H-benzo[f]chromen-1-yl) methyl N,N-dimethylcarbamdithioate have been presented and the calculated structural parameters and energetic properties have been compared with the available X-ray diffraction data. The vibrational frequencies have been calculated using optimized geometry of the molecule. The conformational properties of the molecule have been determined by computing molecular energy properties, in which torsional angle varied from -180° to $+180^\circ$ in steps of 10° . Moreover, natural bond orbital analysis and atomic charge analysis have been performed. Besides, HOMO and LUMO energies have been calculated and their pictures have been presented. Finally, molecular electrostatic potential and thermodynamic properties have been calculated. It is seen that the obtained theoretical results agree well with the available experimental values. In all the calculations, except for optimization and vibrational calculations, B3LYP level of theory with 6-311++G(d,p) basis set has been used.

Keywords: *chromene; DFT; HF; NBO; HOMO; LUMO*

1. Introduction

Privileged structures or scaffolds were first studied by Evans et al. [1]. These structures can bind to a diverse range of targets with high affinities, thus enabling discovery of novel bioactive agents. Chromenes (benzopyrans) represent an important type of privileged structures appearing in natural compounds and they possess interesting biological activities such as antitumor [2], antivasular [3], antimicrobial [4], antioxidant [5], TNF- α inhibitor [6], antifungal [7], anticoagulant [8], estrogenic [9], antiviral [10], anticancer [11, 12], anti-HIV [13], antitubercular [14], anti-inflammatory [15] and anticonvulsant [16, 17]. Benzopyran derivatives are also used in the production of highly effective fluorescent

dyes for synthetic fibers, daylight fluorescent pigments and electrophotographic and electroluminescent devices [18–23].

In the literature, coumarin compound, (3-Oxo-3H-benzo[f]chromen-1-yl) methyl N,N-dimethylcarbamdithioate was synthesized by Kumar et al. [21]. This compound was characterized by X-ray diffraction method and its structure was clarified with ¹H NMR and IR spectra by Mahabaleshwaraiah et al. [24]. To our knowledge, despite the importance mentioned above, there is a lack of theoretical calculations of conformational, natural bond orbital (NBO), molecular geometry, vibrational modes, molecular frontier orbital energy, electronic and thermodynamic properties of the title compound.

The aim of the this work is to to perform Mulliken population, natural population and conformational analyses as well as to describe and

*E-mail: meryem.evecen@amasya.edu.tr

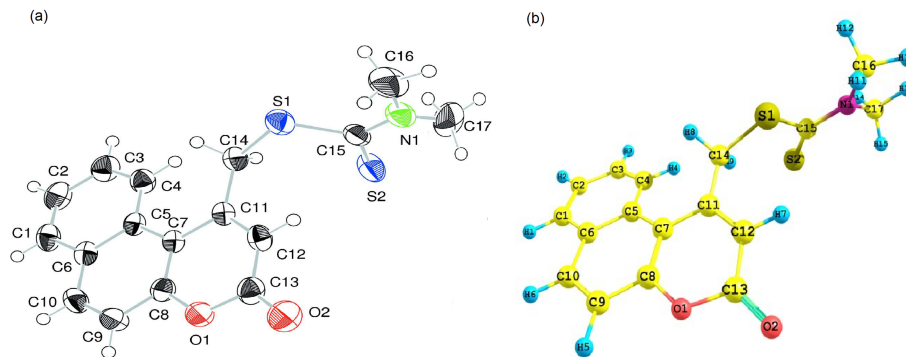


Fig. 1. (a) experimental structure [24], (b) optimized geometric structure of (3-Oxo-3H-benzo[f]chromen-1-yl) methyl N,N-dimethylcarbamodithioate compound (obtained at B3LYP/6-311++G(d,p) level). Visualization of this structure has been carried out with ChemCraft software [27].

characterize the molecular structure, vibrational frequencies, NBO, molecular frontier orbital energies (HOMO and LUMO), molecular electrostatic potential maps (MEP) and thermodynamic properties of (3-Oxo-3H-benzo[f]chromen-1-yl) methyl N,N-dimethylcarbamodithioate compound, using DFT (B3LYP, B3PW91) and HF calculations.

2. Computational methods

The initial molecular geometry of the studied molecule was taken from X-ray diffraction results [24] without any constraints. The geometry optimization is the basic building block of theoretical calculations. Therefore, we made geometry optimization for this molecule by HF and DFT (B3LYP and B3PW91) methods with 6-311++G(d,p) basis sets. Gaussian 09W program package was used in the HF and DFT calculations for the title compound [25]. The harmonic frequency calculations were performed at both HF and DFT levels with 6-311++G(d,p) basis sets using the optimized structural parameters. The obtained vibrational frequencies were scaled by a factor of 0.89 for HF, 0.96 for B3LYP and 0.957 for B3PW91. Vibrational band assignments were made using the Gauss-View molecular visualisation program [26]. In addition, electronic properties, such as natural bond orbital (NBO), charge analysis, HOMO-LUMO energies, and thermodynamic properties were calculated using DFT/B3LYP method.

3. Results and discussion

3.1. Molecular structure

The crystal structure of $C_{17}H_{15}NO_2S_2$ is monoclinic and its space group is P_21/n . The crystal structure parameters of the compound are $a = 14.1575(2) \text{ \AA}$, $b = 6.9399(1) \text{ \AA}$, $c = 15.9750(2) \text{ \AA}$, $\beta = 101.591(1)^\circ$, $\gamma = 78.842(1)^\circ$ and $V = 1537.56(4) \text{ \AA}^3$ [24]. In this molecule, the 3H-benzo[f]-chromene ring system is distinctly twisted. The experimental structural parameters of the novel molecule are as follows: the dihedral angle between the pyran ring and its opposite benzene ring is $9.11(8)^\circ$, the N,N-dimethylcarbamodithioate residue lies almost perpendicular to the pyran ring (dihedral angle = $85.15(7)^\circ$).

The molecular structure of the title compound has been optimized by GAUSSIAN 09W at HF and DFT levels using X-ray diffraction experimental data [24] without any constraints and is shown in Fig. 1 with atomic numbers [27]. The energies of the optimized structure obtained by HF, DFT-B3LYP and DFT-B3PW91 methods are -44951.761 eV , -45136.013 eV and -5124.020 eV , respectively. Selected comparative structural parameters obtained from the optimization are presented in Table 1.

Table 1. Selected molecular structure parameters.

Parameters	Experimental [24]	This work (theoretical)		
		HF	B3LYP	B3PW91
Bond lengths [Å]				
S1-C15	1.784	1.786	1.815	1.801
S1-C14	1.800	1.812	1.825	1.811
S2-C15	1.664	1.668	1.669	1.663
O1-C13	1.367	1.346	1.394	1.388
O1-C8	1.374	1.345	1.358	1.351
O2-C13	1.207	1.181	1.204	1.202
N1-C15	1.327	1.328	1.350	1.346
N1-C16	1.460	1.464	1.467	1.458
N1-C17	1.465	1.465	1.468	1.459
C1-C2	1.356	1.359	1.374	1.372
C5-C6	1.424	1.413	1.434	1.431
C5-C7	1.453	1.454	1.452	1.447
C7-C8	1.387	1.371	1.398	1.396
C11-C14	1.514	1.519	1.517	1.511
Bond angles [°]				
C15-S1-C14	103.500	105.175	102.903	102.453
C13-O1-C8	121.630	123.410	122.528	122.536
C15-N1-C17	120.920	119.243	119.007	118.851
C16-N1-C17	114.640	117.995	117.790	118.072
C5-C7-C11	127.610	127.834	127.389	127.293
O1-C8-C7	123.370	123.504	123.182	123.250
C12-C11-C14	119.090	120.287	119.832	119.858
O2-C13-O1	117.550	119.135	117.975	117.952
O1-C13-C12	115.970	115.104	114.576	114.616
C11-C14-S1	116.430	117.221	116.547	116.222
N1-C15-S1	113.330	113.256	112.548	112.569
S2-C15-S1	122.510	122.956	123.816	123.961
Torsion angles [°]				
C6-C5-C7-C11	-171.940	-170.465	-168.549	-168.067
C5-C7-C8-O1	176.450	174.828	173.503	173.426
C8-O1-C13-O2	-176.030	-172.990	-172.990	-172.832
C7-C11-C14-S1	158.210	158.877	155.798	155.586
C15-S1-C14-C11	86.480	97.353	105.834	107.283
C16-N1-C15-S2	178.010	178.745	177.490	177.353
C17-N1-C15-S1	-179.390	-177.760	-175.282	-175.203
C14-S1-C15-N1	-173.890	-178.865	-176.895	-176.664

Table 2. Comparison of the experimental and calculated vibrational frequencies [cm^{-1}].

Assignments	Experimental [24]	HF	B3LYP	B3PW91
ν (C–H) R s	–	2984	3063	3064
ν (C–H) R as	–	2972	3048	3048
ν (C–H ₃) as	–	2949	3021	3022
ν (C–H ₃) as	–	2914	3009	2980
ν (C–H ₃) s	–	2883	2920	2916
ν (C–H ₃) s	–	2852	2903	2900
ν (C–H ₂) s	–	2838	2866	2824
ν (C=O)	1708.6	1766	1728	1744
ν (C=C) R	–	1628	1591	1601
ν (C–C) R	–	1586	1580	1588
ν (C=C) R	–	1548	1517	1527
ν (C=C) R	–	1488	1488	1491
ω (C–H ₃)	–	1480	1471	1467
γ (C–H)	–	1436	1426	1425
ν (C=C) R + ω (C–H ₂)	–	1367	1366	1355
ν (C–N) + ω (C–H ₃) + ν (C–O)	–	1344	1341	1347
ω (C–H ₂) + ν (C–C) R + ν (C–N)	–	1337	1337	1329
ν (C–C) R + ω (C–H ₂)	–	1255	1313	1288
ν (C–O–C)	1279	1195	1290	1258
ν (C–N) + ν (C=S)	1251	1137	1233	1244
δ (C–H ₃) + δ (C–H ₂)	–	1030	1223	1179
Ω (C–H ₂) + α (C–H) R	–	1011	1169	1166
ν (C–O) + α (C–H)	–	962	1106	1131
γ (C–H ₃)	–	957	1025	1123
Ω (C–H ₂) + α (C–H) R	–	907	973	1088
ν (C–O)	1036	904	967	979
δ (C–H)	–	856	940	953
ν (C–N) + ν (C–S) + ω (C–H ₂)	–	834	951	967
ν (C–O) R	–	750	874	880
ν (C–N) + ν (C–S)	842	740	831	848
ω (C–H) R	–	717	799	796
ω (C–H) R+ ν (S–CH ₂)	–	572	727	752
ν (C–S)	660	560	672	563
γ (C–H ₂)	–	432	365	366

ν – stretching; δ – twisting; γ – rocking; ω – wagging; α – scissoring; s – symmetric; as – asymmetric; R – ring.

Taking into account these results we can conclude that B3LYP/6-311++G(d,p) method can be used as the main reference. It is also well known from the literature that DFT-optimized bond lengths are usually longer and more accurate than HF due to the electron correlation included in DFT [28].

The bond lengths, angles and dihedral angles are presented in Table 1. It is seen from the Table that the calculated bond lengths are slightly larger than the corresponding experimental values. This discrepancy may originate from the fact that the theoretical calculations were performed for the gaseous phase whereas the experimental results

were obtained for the solid phase [29]. Another reason can be the change in charge distribution on the carbon atom of the benzene ring [30]. The carbon-hydrogen bond lengths are given as standard values during the solvation of the crystal structure by SHELXS97 [31, 32]. In Table 1, we did not give them because of the discrepancies in the bond lengths between carbon and hydrogen atoms.

From Table 1 we can see that the calculated bond angles are in agreement with the experimental results. The only discrepancy occurs for the angle C16-N1-C17, which we think may originate from sharp in-plane and out-of-plane vibrations of the methyl group bonded to nitrogen atom. We also see that all the calculated dihedral angles are in a good agreement with the experimental results.

The calculated geometrical parameters obtained by HF, DFT/B3LYP and DFT/B3PW91 methods represent a good approximation and they are the bases for calculating other parameters, such as vibrational frequencies, conformational analysis, frontier molecular orbitals, electronic and thermodynamic properties.

3.2. Vibrational spectra

Harmonic vibrational frequencies were calculated using HF, DFT/B3LYP and DFT/B3PW91 with the 6-311++G(d,p) basis set. Stimulated IR spectra of the title compound are shown in Fig. 2. The calculated and available experimental frequencies of the IR spectra of the title compound are presented in Table 2 with probable assignments obtained by the use of Gauss-View molecular visualization program. Theoretical vibrational frequencies of the title compound obtained by the three methods agree well with experimental data.

The studied title compound $C_{17}H_{15}NO_2S_2$ includes 37 atoms and therefore undergoes 105 normal modes of vibrations. For fitting the theoretical wavenumbers to the experimental ones, an overall scaling factor has been introduced by using a least-square optimization of the computed values to the experimental ones. Vibrational frequencies have been scaled as 0.890, 0.960 and

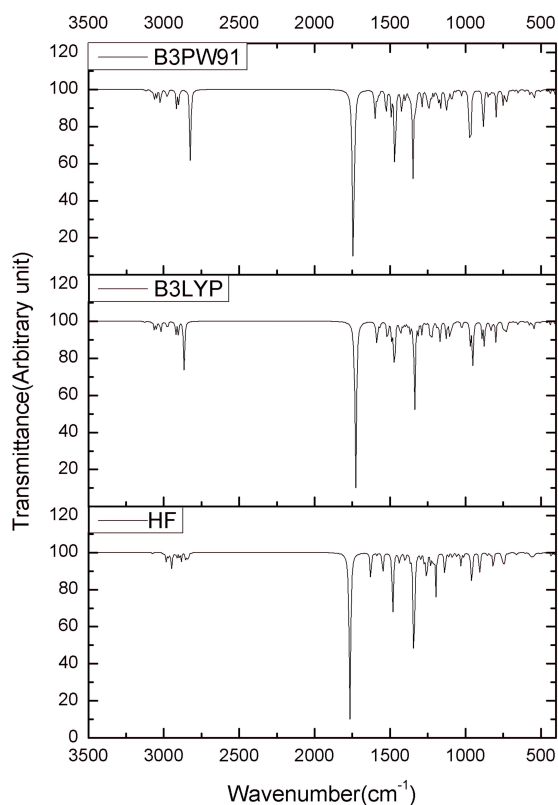


Fig. 2. Calculated FT-IR spectrum of (3-Oxo-3H-benzo[f]chromen-1-yl) methyl N,N-dimethylcarbamodithioate compound.

0.957 for HF, B3LYP and B3PW91, respectively, with 6-311++G(d,p) basis set [33, 34].

The IR spectra contain some characteristic bands of the stretching vibrations of C–H, C–H₃, C–H₂, C=O, C–O, C–C, C–N and C–S groups, which were analysed in a detailed way.

Among the vibrations in molecules, the C–H vibration has a well-known characteristic frequency, and in the region of 3100 cm^{-1} to 3000 cm^{-1} , which is the region characteristic for ready identification of C–H stretching vibrations in plane, multiple weak bands are expected for aromatic compounds [35]. The bands in this region are not affected by the nature of the substituents.

Looking at Table 2, we see that the calculated C–H aromatic stretching intensities have a medium intensity and the results obtained by three different methods are 2984 cm^{-1} to 2972 cm^{-1}

for HF, 3063 cm^{-1} to 3048 cm^{-1} for B3LYP and 3064 cm^{-1} to 3048 cm^{-1} for B3PW91. As can be seen, these intensities are in the expected region. It is known that C–H in-plane and out-of-plane bending vibrations lie in the range of 1300 cm^{-1} to 1000 cm^{-1} and 950 cm^{-1} to 800 cm^{-1} [36–38]. We have calculated four C–H in-plane bending vibrations of the title compound by three different methods as 1436 cm^{-1} , 1011 cm^{-1} , 962 cm^{-1} and 907 cm^{-1} by HF; 1426 cm^{-1} , 1169 cm^{-1} , 1106 cm^{-1} and 973 cm^{-1} by B3LYP, and 1425 cm^{-1} , 1166 cm^{-1} , 1131 cm^{-1} and 1088 cm^{-1} by B3PW91. An out-of-plane twisting-bending mode has been calculated at 856 cm^{-1} by HF, 940 cm^{-1} by B3LYP and 953 cm^{-1} by B3PW91 and two out-of-plane waggings have been calculated at 717 cm^{-1} and 572 cm^{-1} by HF, 799 cm^{-1} and 727 cm^{-1} by B3LYP and 796 cm^{-1} and 752 cm^{-1} by B3PW91.

The studied title compound has two C–H₃ groups. The C–H methyl group stretching vibrations, especially observed in the range of 3000 cm^{-1} to 2900 cm^{-1} , are highly localized [39, 40]. In this study, the asymmetric bands with high peaks have been found at 2949 cm^{-1} and 2914 cm^{-1} by HF, 3021 and 3009 cm^{-1} by B3LYP and 3022 cm^{-1} and 2980 cm^{-1} by B3PW91, while symmetric stretching vibrations have been found at 2883 cm^{-1} and 2852 cm^{-1} by HF, 2920 cm^{-1} and 2903 cm^{-1} by B3LYP and 2916 cm^{-1} and 2900 cm^{-1} by B3PW91. In this investigation, two C–H₃ wagging vibrations have been found at 1480 cm^{-1} and 1344 cm^{-1} by HF, 1471 cm^{-1} and 1341 cm^{-1} by B3LYP and 1467 cm^{-1} and 1347 cm^{-1} by B3PW91. The twisting-bending mode have been found at 1030 cm^{-1} by HF, 1223 cm^{-1} by B3LYP, and 1179 cm^{-1} by B3PW91. We have observed rocking frequency at 957 cm^{-1} by HF, 1025 cm^{-1} by B3LYP and 1123 cm^{-1} by B3PW91, which is in agreement with the literature [41, 42].

In this work, six wagging and one stretching, twisting and rocking methylene vibrations are observed. Generally, the symmetric C–H₂ stretching vibrations are observed between 3000 cm^{-1} and 2900 cm^{-1} [43]. In accordance with this, C–H₂

symmetric mode has been found at 2838 cm^{-1} by HF, 2866 cm^{-1} by B3LYP and 2824 cm^{-1} by B3PW91. Six C–H₂ wagging out-of-plane deformation vibrations have been obtained at 1367 cm^{-1} , 1337 cm^{-1} , 1255 cm^{-1} , 1011 cm^{-1} , 907 cm^{-1} and 834 cm^{-1} by HF; 1366 cm^{-1} , 1337 cm^{-1} , 1313 cm^{-1} , 1169 cm^{-1} , 973 cm^{-1} and 951 cm^{-1} by B3LYP, and 1355 cm^{-1} , 1329 cm^{-1} , 1288 cm^{-1} , 1166 cm^{-1} , 1088 cm^{-1} and 967 cm^{-1} by B3PW91. Twisting and rocking bands are observed at 1030 cm^{-1} and 432 cm^{-1} by HF, 1223 cm^{-1} and 365 cm^{-1} by B3LYP and 1179 cm^{-1} and 366 cm^{-1} by B3PW91.

These vibrations are more effective for analyzing various factors in ring aromatic compounds. Because of different electronegativities of C and O, the C=O bond reduces the frequencies of the C=O stretching absorption to a greater degree than intermolecular H bonding does. The lone pair of electrons on oxygen also determines the nature of the carbonyl groups. The C=O vibration appearing in the expected range shows that it is not much affected by other vibrations, as mentioned in literature [44]. As is well-known, compounds including carbonyl group, show C=O stretching vibrations in the region 1920 cm^{-1} to 1640 cm^{-1} . In the present study, C=O strong stretching vibration has been identified at 1766 cm^{-1} by HF, 1728 cm^{-1} by B3LYP, and at 1744 cm^{-1} by B3PW91, which is in the expected region [45] and in good agreement with the experimental value of 1708.6 cm^{-1} (Table 2).

C–O stretching band of the aromatic ring in IR spectrum is characterized by the frequencies around 1270 cm^{-1} to 1230 cm^{-1} [46]. For aromatic rings, the C–O vibrations are observed at 1195 cm^{-1} (1290 cm^{-1} , 1258 cm^{-1}) and 904 cm^{-1} (967 cm^{-1} , 979 cm^{-1}) by HF (B3LYP, B3PW91) method. These assignments were also supported by the experimental values of 1279 cm^{-1} and 1036 cm^{-1} .

The C–N stretching vibrations are observed in 1382 cm^{-1} to 1266 cm^{-1} [45], 1150 cm^{-1} to 1120 cm^{-1} [47], and 1248 cm^{-1} to 1199 cm^{-1} [48]. In this study, we have observed the C–N stretching vibrations at

1344 cm^{-1} , 1337 cm^{-1} , 1137 cm^{-1} , 834 cm^{-1} and 740 cm^{-1} by HF; 1341 cm^{-1} , 1337 cm^{-1} , 1233 cm^{-1} , 951 cm^{-1} and 831 cm^{-1} by B3LYP; and 1347 cm^{-1} , 1329 cm^{-1} , 1244 cm^{-1} , 967 cm^{-1} and 848 cm^{-1} by B3PW91. These results are in the expected region and agree well with the experimental result 842 cm^{-1} (Table 2).

The aromatic stretching vibrations are very prominent, as the involved double C=C bond is in conjugation with the ring. The ring C=C and C-C stretching vibrations were observed in the region of 1620 cm^{-1} to 1390 cm^{-1} by Arivazhagan *et al.* [49] and in the region of 1625 cm^{-1} to 1280 cm^{-1} by Varasanyi *et al.* [50]. In the present work, we have observed ring C=C and C-C stretching vibration frequencies at 1628 cm^{-1} , 1586 cm^{-1} , 1548 cm^{-1} , 1488 cm^{-1} , 1367 cm^{-1} , 1337 cm^{-1} and 1255 cm^{-1} by HF, 1591 cm^{-1} , 1580 cm^{-1} , 1517 cm^{-1} , 1488 cm^{-1} , 1366 cm^{-1} , 1337 cm^{-1} and 1313 cm^{-1} by B3LYP, and 1601 cm^{-1} , 1588 cm^{-1} , 1527 cm^{-1} , 1491 cm^{-1} , 1355 cm^{-1} , 1329 cm^{-1} and 1288 cm^{-1} by B3PW91.

The absorption bands of C=S group were observed by Silverstein *et al.* in the region of 1563 cm^{-1} to 700 cm^{-1} [51] and the absorption bands of C-S group were found in the range of 930 cm^{-1} to 670 cm^{-1} with a moderate intensity [52, 53]. The experimental C=S vibration mode was observed at 1251 cm^{-1} while C-S vibration modes were at 842 cm^{-1} and 660 cm^{-1} [24]. In this work, we have calculated C=S vibrations at 1137 cm^{-1} , 1233 cm^{-1} and 1244 cm^{-1} by HF, B3LYP and B3PW91, respectively, while C-S vibrations were obtained at 834 cm^{-1} , 740 cm^{-1} , 572 cm^{-1} and 560 cm^{-1} by HF; 951 cm^{-1} , 831 cm^{-1} , 727 cm^{-1} and weak intensity 672 cm^{-1} by B3LYP; and 967 cm^{-1} , 848 cm^{-1} , 752 cm^{-1} and 563 cm^{-1} by B3PW91. The calculated results showed slight deviations from experimental values due to hydrogen bonding interactions. We can say that these vibrations coincide satisfactorily with the literature and experimental values (Table 2).

FT-IR spectrum of the title compound has been obtained by HF, B3LYP and B3PW91 methods, and is shown in Fig. 2. It can be concluded from Fig. 2 and Table 2 that except for HF method, other

methods give the results which are in good agreement with each other and the experiment. The exception for HF may be due to the fact that HF takes no electron correlation into account. It is seen from Table 2 that the calculated vibrational frequencies of the title compound agree well with the available experimental results. From this, we can conclude that other vibrational frequencies presented in this work can be a reference for experimentalists.

3.3. Conformational analysis

In order to define the preferential position of low energy structures, computations were performed using B3LYP/6-311++G(d,p) as a function of selected degrees of torsional freedom T(C11-C14-S1-C15). The respective value of selected degrees of torsional freedom, T(C11-C14-S1-C15), is 86.48° in X-ray structure [24], whereas the corresponding value in DFT optimized geometry is 105.834°. In Fig. 3, the molecular energy profiles with respect to rotations about the selected torsion angles are shown. It is seen from Fig. 3 that the low energy domains for T(C11-C14-S1-C15) are located at 70° and 180°. Energy difference between the most favorable and unfavorable conformers is calculated as 1.56 eV, when selected degree of torsional freedom is considered.

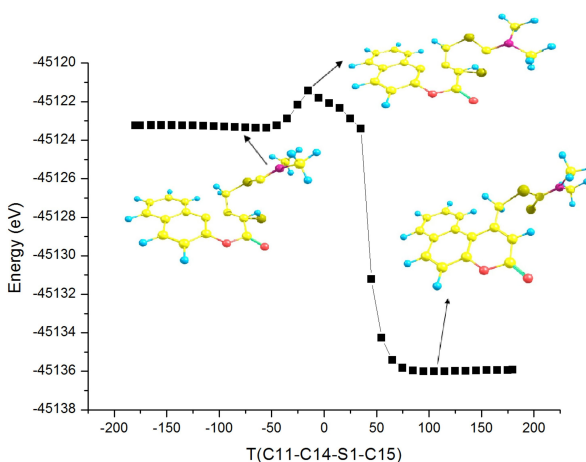


Fig. 3. Potential energy profile obtained using B3LYP/6-311++G(d,p) method for the internal rotation around the C14-S1 bond of (3-Oxo-3H-benzo[f]chromen-1-yl) methyl N,N-dimethylcarbomodithioate compound.

It must be noted that the selected torsion angle in the crystal structure of the title compound is near to its global minimum value.

3.4. Natural bond orbital analysis

In order to investigate charge transfer or conjugative interaction in molecular systems, we have executed natural bond orbital (NBO) analysis using Gaussian 09W program. Some electron donor orbitals, acceptor orbitals and the interacting stabilization energy resulting from the second-order micro-disturbance theory have been reported in the literature [54, 55].

More intensive interactions between electron donors and electron acceptors depend on larger $E^{(2)}$ value, i.e. the more donating tendency from electron donors to electron acceptors, the greater the extent of conjugation of the whole system [56]. The stabilization energy $E^{(2)}$ associated with $i(\text{donor}) \rightarrow j(\text{acceptor})$ delocalization is obtained by [57, 58]:

$$E^{(2)} = -q_i \frac{(F_{ij})^2}{\epsilon_j - \epsilon_i} \quad (1)$$

where q_i is the donor orbital occupancy, ϵ_i , ϵ_j are orbital energies and F_{ij} is the off-diagonal NBO Fock matrix element. For investigating the intramolecular interactions, second-order perturbation theory was used for obtaining stabilization energies of the title compound. We found from the NBO analysis that the intramolecular interactions formed by the orbital overlap between bonding (C–S), (C–O), (C–N), (C–C) and (C–H) and anti-bonding (C–O), (C–N), (C–C) and (C–H) orbitals resulting from intramolecular charge transfer, cause stabilization of the compound. Selected second-order perturbation energies $E^{(2)}$ associated with $i \rightarrow j$ delocalization in gas phase have been tabulated in Table 3. The stabilization energies larger than 300 kcal/mol have been listed in the table presented in the literature [59]. In electron density (ED), these interactions are observed as an increase in (C–S), (C–C) and (C–O) anti-bonding orbital that weakens the respective bonds. The electron density of dimethylamino fragment (~ 1.99 e) demonstrates clearly the strong delocalization. Additionally, the ED of conjugated bond of 3H-chromene ring (~ 1.98 e) shows clearly a strong delocalization inside the compound [59].

Table 3. Selected second-order perturbation energies $E^{(2)}$ associated with $i \rightarrow j$ delocalization in gas phase.

Donor orbital (i)	Type	ED/e	Acceptor orbital (j)	Type	ED/e	$E^{(2)}$ [kcal/mol] ^a	$E(j) - E(i)$ [a.u.] ^b	$F(i,j)$ [a.u.] ^c
S1-C15	σ	1.97580	C8-C9	σ^*	0.02256	634.30	0.03	0.127
S2-C15	σ	1.98331	C8-C9	σ^*	0.02256	1495.44	0.12	0.376
S2-C15	σ	1.98331	C16-H11	σ^*	0.01111	718.46	0.30	0.412
N1-C15	σ	1.98913	C8-C9	σ^*	0.02256	729.01	0.25	0.386
N1-C15	σ	1.98913	C16-H11	σ^*	0.01111	1001.38	0.43	0.587
N1-C16	σ	1.98641	C8-C9	σ^*	0.02256	872.35	0.13	0.303
N1-C16	σ	1.98641	C16-H11	σ^*	0.01111	572.41	0.31	0.376
N1-C17	σ	1.98352	C8-C9	σ^*	0.02256	3068.96	0.06	0.377
N1-C17	σ	1.98352	C16-H11	σ^*	0.01111	3399.96	0.24	0.800
C1-C2	σ	1.97713	C5-C6	π^*	1.55092	1355.02	0.12	0.409
C1-C2	σ	1.97713	C8-C9	σ^*	0.02256	541.72	0.23	0.318

C1-C2	σ	1.97713	C16-H11	σ^*	0.01111	343.71	0.41	0.337
C11-C12	π	1.80618	O2-C13	σ^*	0.01287	2130.49	1.54	1.694
C11-C12	π	1.80618	N1-C17	σ^*	0.02186	461.80	2.40	0.984
C11-C12	π	1.80618	C1-C6	σ^*	0.02327	592.10	2.54	1.144
C11-C12	π	1.80618	C2-H2	σ^*	0.01389	21144.90	0.34	2.504
C11-C12	π	1.80618	C3-C4	σ^*	0.01442	3335.32	1.36	1.990
C11-C12	π	1.80618	C5-C6	π^*	1.55092	934.01	1.87	1.268
C11-C12	π	1.80618	C6-C10	σ^*	0.02324	569.48	2.58	1.132
C11-C12	π	1.80618	C8-C9	σ^*	0.02256	1527.07	1.98	1.625
C11-C12	π	1.80618	C11-C12	σ^*	0.01946	303.11	2.60	0.829
C11-C12	π	1.80618	C11-C12	π^*	0.17312	414.77	2.25	0.867
C11-C12	π	1.80618	C14-H9	σ^*	0.04360	644.07	2.32	1.133
C11-C12	π	1.80618	C16-H11	σ^*	0.01111	1717.75	2.16	1.805
C11-C12	π	1.80618	C17-H14	σ^*	0.01317	1071.97	3.38	1.781
C16-H10	σ	1.98990	C5-C6	π^*	1.55092	393.95	0.34	0.371
C16-H10	σ	1.98990	C8-C9	σ^*	0.02256	1719.49	0.45	0.790
C16-H10	σ	1.98990	C16-H11	σ^*	0.01111	1906.38	0.63	0.979
C17-H13	σ	1.99069	C11-C12	π^*	0.17312	405.51	0.18	0.254
C17-H13	σ	1.99069	C14-H9	σ^*	0.04360	319.46	0.25	0.254
C17-H13	σ	1.99069	C16-H11	σ^*	0.01111	5450.36	0.10	0.648
C17-H14	σ	1.98811	C11-C12	π^*	0.17312	431.89	0.17	0.251
C17-H14	σ	1.98811	C14-H9	σ^*	0.04360	341.72	0.23	0.255
C17-H14	σ	1.98811	C16-H11	σ^*	0.01111	5664.53	0.08	0.609
C17-H14	σ	1.98811	C17-H14	σ^*	0.01317	257.49	1.30	0.516
C17-H15	σ	1.98787	C1-C6	σ^*	0.02327	1140.73	0.04	0.186
C17-H15	σ	1.98787	C6-C10	σ^*	0.02324	1422.13	0.09	0.315
C17-H15	σ	1.98787	C11-C12	σ^*	0.01946	1017.78	0.10	0.281
S1	LP(1)	1.97153	C8-C9	σ^*	0.02256	342.86	0.02	0.081
S2	LP(1)	1.97746	C8-C9	σ^*	0.02256	1656.20	0.10	0.360
S2	LP(1)	1.97746	C16-H11	σ^*	0.01111	496.22	0.28	0.331
S2	LP(3)	1.52194	C15	LP*(1)	0.98014	563.69	0.02	0.108
O2-C13	π^*	0.29368	C1-H1	σ^*	0.01414	659.94	24.67	9.181
O2-C13	π^*	0.29368	C2-H2	σ^*	0.01389	542.04	25.08	8.392
O2-C13	π^*	0.29368	C3-C4	σ^*	0.01442	371.63	26.09	7.082
O2-C13	π^*	0.29368	C3-C4	π^*	0.27123	3841.97	19.48	14.530
O2-C13	π^*	0.29368	C5-C6	π^*	1.55092	400.08	26.61	4.740

O2-C13	π^*	0.29368	C17-H14	σ^*	0.01317	302.73	28.12	6.649
O2-C13	π^*	0.29368	C17-H15	σ^*	0.01164	2690.23	18.61	16.166
C3-C4	π^*	0.27123	C1-H1	σ^*	0.01414	774.37	5.19	4.739
C3-C4	π^*	0.27123	C2-H2	σ^*	0.01389	686.92	5.60	4.636
C3-C4	π^*	0.27123	C3-C4	σ^*	0.01442	359.12	6.61	3.640
C3-C4	π^*	0.27123	C5-C6	π^*	1.55092	342.60	7.13	2.305
C5-C6	π^*	0.46141	N1-C17	σ^*	0.02186	300.63	0.53	0.726
C5-C6	π^*	0.46141	C8-C9	σ^*	0.02256	1480.79	0.11	0.740
C5-C6	π^*	0.46141	C9-C10	π^*	0.23065	306.38	0.52	0.603
C5-C6	π^*	0.46141	C11-C12	σ^*	0.01946	346.70	0.72	0.911
C5-C6	π^*	0.46141	C11-C12	π^*	0.17312	473.47	0.38	0.669
C5-C6	π^*	0.46141	C14-H9	σ^*	0.04360	570.34	0.44	0.893
C5-C6	π^*	0.46141	C16-H11	σ^*	0.01111	1108.24	0.29	1.041
C9-C10	π^*	0.23065	N1-C17	σ^*	0.02186	1285.15	0.02	0.359
C11-C12	π^*	0.17312	C11-C12	σ^*	0.01946	499.63	0.07	0.492

^aE⁽²⁾, energy of hyper-conjugative interactions.

^bEnergy difference between donor and acceptor i and j NBO orbitals.

^cF_{ij} is the Fock matrix element between i and j NBO orbitals.

The hyperconjugative interactions of $\sigma \rightarrow \sigma^*$ and $\sigma \rightarrow \pi^*$ occur in various bonds in the compound. As an example, the hyperconjugative interactions of $\sigma(\text{N1-C15})$ distribute to $\sigma^*(\text{C16-H11})$, $\sigma^*(\text{C1-C6})$, $\sigma^*(\text{C8-C9})$ and $\pi^*(\text{C11-C12})$. In case of $\sigma(\text{C16-H10})$ orbital, the $\sigma^*(\text{C8-C9})$ and $\sigma^*(\text{C16-H11})$ show stabilization energy of 1719.49 kcal/mol and 1906.38 kcal/mol. Also for $\sigma(\text{C17-H13})$ and $\sigma(\text{C17-H14})$ orbitals, the $\sigma^*(\text{C16-H11})$ show stabilization energy of 5450.36 kcal/mol and 5664.53 kcal/mol, respectively. The intramolecular hyperconjugative interactions of $\sigma(\text{C17-H15})$ distribute to the $\sigma^*(\text{C1-C6})$, $\sigma^*(\text{C6-C10})$ and $\sigma^*(\text{C11-C12})$ resulting in a stabilization of 1140.73 kcal/mol, 1422.13 kcal/mol and 1017.78 kcal/mol.

The other hyperconjugative interaction of the $\sigma(\text{C1-C2})$ enhanced further conjugate with antibonding orbital of $\pi^*(\text{C5-C6})$ and $\sigma^*(\text{C6-C10})$ which results in strong delocalizations of 1355.02 kcal/mol and 141.88 kcal/mol, respectively.

In addition, the $\pi^*(\text{O2-C13})$ NBO conjugates with respective bonds of $\pi^*(\text{C3-C4})$ and

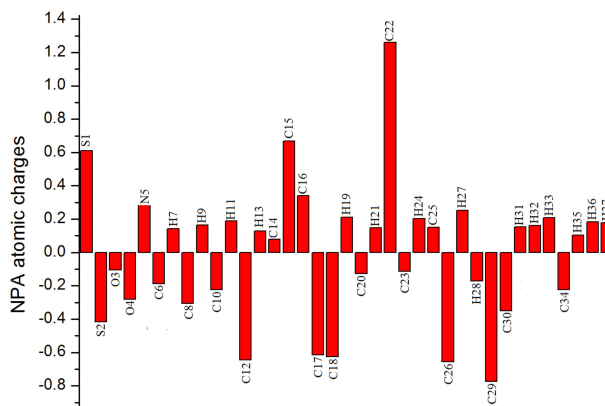


Fig. 4. Natural charges of (3-Oxo-3H-benzo[f]chromen-1-yl) methyl N,N-dimethylcarbamodithioate compound.

$\sigma^*(\text{C17-H15})$ result in an enormous stabilization of 3841.97 kcal/mol and 2690.23 kcal/mol, respectively. The $\pi^*(\text{C5-C6})$ bond interacts with $\sigma^*(\text{C8-C9})$ and $\sigma^*(\text{C16-H11})$ with energies of 1480.79 kcal/mol and 1108.24 kcal/mol, respectively. This enhances further conjugate with antibonding orbital from $\pi^*(\text{C9-C10}) \rightarrow \sigma^*(\text{N1-C17})$, which results in strong delocalization of 1285.15 kcal/mol.

Table 4. Atomic charge of the title compound in gas phase and solution phase.

Atom	In gas phase		In solution phase B3LYP		
	B3LYP	chloroform ($\epsilon = 4.71$)	ethanol ($\epsilon = 24.55$)	DMSO ($\epsilon = 46.82$)	water ($\epsilon = 78.36$)
S1	0.60956	0.537027	0.478449	0.475604	0.474265
S2	-0.41615	-0.478779	-0.517133	-0.521399	-0.523617
O1	-0.10548	-0.117913	-0.122201	-0.122873	-0.123183
O2	-0.28113	-0.357899	-0.385822	-0.389277	-0.390891
N1	0.28536	0.298592	0.307627	0.309635	0.310459
C1	-0.18763	-0.211948	-0.230014	-0.231313	-0.231804
H1	0.14204	0.167190	0.176634	0.177789	0.178326
C2	-0.30524	-0.340560	-0.360467	-0.361857	-0.362547
H2	0.16439	0.185189	0.192497	0.193424	0.193855
C3	-0.22452	-0.215689	-0.188075	-0.186689	-0.186009
H3	0.18804	0.208438	0.216478	0.217452	0.217904
C4	-0.64326	-0.669077	-0.687328	-0.688431	-0.688799
H4	0.12792	0.146120	0.142398	0.142554	0.142555
C5	0.08003	0.062580	0.053604	0.052257	0.051574
C6	0.66788	0.642047	0.626788	0.625929	0.625547
C7	0.34132	0.366547	0.382597	0.382524	0.382460
C8	-0.61457	-0.623369	-0.655181	-0.656349	-0.656935
C9	-0.62482	-0.662370	-0.683429	-0.684688	-0.685298
H5	0.21109	0.225034	0.229047	0.229527	0.229749
C10	-0.12789	-0.135643	-0.121869	-0.121684	-0.121666
H6	0.14697	0.174296	0.184445	0.185690	0.186265
C11	1.26064	1.321272	1.340740	1.341024	1.341092
C12	-0.11441	-0.128612	-0.131286	-0.132754	-0.133329
H7	0.20208	0.194343	0.180341	0.179997	0.179778
C13	0.14974	0.178211	0.174948	0.176519	0.177132
C14	-0.65621	-0.600780	-0.524466	-0.519846	-0.517605
H8	0.25195	0.260395	0.262317	0.263060	0.263432
H9	-0.17049	-0.124575	-0.065318	-0.061254	-0.059193
C15	-0.77419	-0.755970	-0.747506	-0.746435	-0.745892
C16	-0.35031	-0.355090	-0.348341	-0.348504	-0.348327
H10	0.15430	0.171636	0.177946	0.178740	0.179087
H11	0.16234	0.171409	0.177508	0.177157	0.177092
H12	0.20873	0.214148	0.211118	0.211960	0.212235
C17	-0.22322	-0.230832	-0.237464	-0.238590	-0.239117
H13	0.10379	0.123579	0.130472	0.131457	0.131906
H14	0.18292	0.181195	0.183180	0.183424	0.183578
H15	0.17838	0.179857	0.176768	0.176222	0.175921

The stronger intramolecular hyper- $\sigma^*(\text{C3-C4})$ (3335.32 kcal/mol), $\sigma^*(\text{C8-C9})$ conjugative interactions of π -electrons (1527.07 kcal/mol), $\sigma^*(\text{C16-H11})$ with the greatest energy contribute to (1717.75 kcal/mol), $\sigma^*(\text{C17-H14})$ $\text{C11-C12} \rightarrow \sigma^*(\text{C2-H2})$ (21144.90 kcal/mol), (1071.97 kcal/mol), $\pi^*(\text{C5-C6})$ (934.01 kcal/mol).

The interaction energy related to the resonance in the present molecule involves electron density transfer from a lone pair of S2 to anti-bonding $\sigma^*(\text{C8-C9})$ of chromene carbon atoms, resulting in an enormous stabilization (up to 1656.20 kcal/mol). The weaker lone pairs of S1, O1, O2 and N1 donate their electrons to the σ , π and LP(1)-type anti-bonding orbital.

We also calculated atomic charge values of the compound by the natural population analysis (NPA) using the DFT/B3LYP method with the 6-311++G (d,p) basis set in order to determine the electron population of each atom in the title compound. The natural charges were obtained by natural bond orbital analysis (NBO). NPA charge distribution is shown in Fig. 4. As can be seen, all hydrogen atoms have a net positive charge. The NPA analysis shows that all carbon atoms are negatively charged, except for C8, C11 and C13 atoms of pyran ring. Among all these atoms, the maximum positive atomic charge is obtained only for C13 atom of carbonyl group. This is due to the attachment of maximum negatively charged C13=O2 double bond.

3.5. Atomic charge distributions in gas-phase and in solution phase

The Mulliken atomic charges [60] for the non-H atoms of the title molecule calculated at the B3LYP/6-311++G(d,p) level in gas-phase are presented in Table 4. To investigate the solvent effect on the atomic charge distribution of the title molecule, PCM method has been used. The results obtained for four selected solvents (chloroform, ethanol, dmsol and water) are listed in Table 4.

The Mulliken atomic charges show that the carbon atoms attached to hydrogen atoms are negative, whereas C5, C6, C7, C11 atoms and C13 (adjacent to the oxygen atoms) are positively charged in the whole phase. The other carbon atoms have more negative atomic charges whereas all the hydrogen atoms have positive charges except for H9. Among all the atoms, the maximum positive atomic charge is obtained only for C11 atom of carbonyl group. This is due to the attachment

of the most negatively charged C14 atom. In the gas phase, S1, C6 and H7 atoms have larger positive atomic charges while C3, C14, H9 and C15 atoms have larger negative atomic charges. This behavior may be the result of electronegativity differences between bonded atoms and the resultant bond character. This method and the NPA analysis predict the same tendencies.

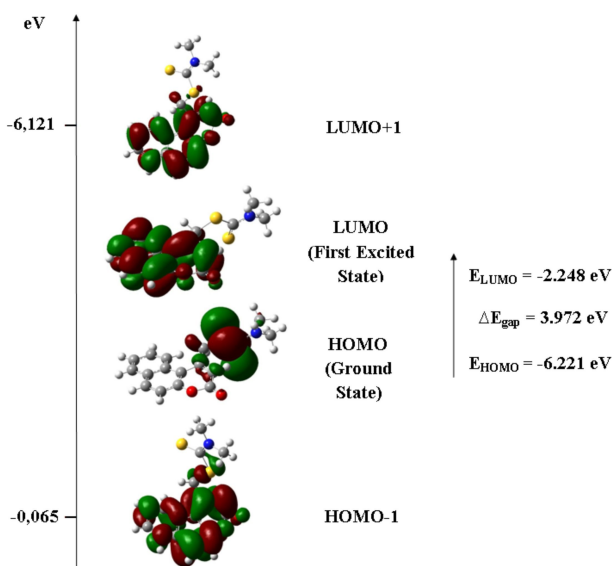


Fig. 5. Molecular orbital surfaces and energy levels (given in parentheses) for the HOMO - 1, HOMO, LUMO and LUMO + 1 of (3-Oxo-3H-benzo[f]chromen-1-yl) methyl N,N-dimethylcarbamodithioate computed at B3LYP/6-311++G(d,p) level.

On the other hand, it has been found that, in solution-phase, the atomic charge values of the S2, O2, N1, C1, C2, C4, C7, C8, C9 and C11 atoms are larger than those in the gas-phase and their atomic charge values increase with the increase in the polarity of the solvent, but the values of S1, C6, H7, C3, C14, H9 and C15 atoms decrease with the increasing polarity of the solvent. The coordination of these atoms is changing in different solvents, which may be helpful when one wishes to use this molecule to construct interesting metal complexes with different coordinate geometries [61].

3.6. Frontier molecular orbital analysis

The frontier molecular orbitals constitute a basic building block in electric and optical properties as well as in UV-Vis spectra and chemical reactions [62]. In this study, we found that the most energetic method is B3LYP with -45136.013 eV energy followed by B3PW91 with -45124.020 eV energy and then HF with -44951.761 eV energy. Fig. 5 shows the distributions and energy levels of the HOMO and LUMO orbitals, computed using the most energetic method (B3LYP) for the title compound. Both HOMOs and the LUMOs are mostly of the π -antibonding type and thus, the electronic transitions from HOMO to LUMO may result from the contribution of π - π^* bands [63].

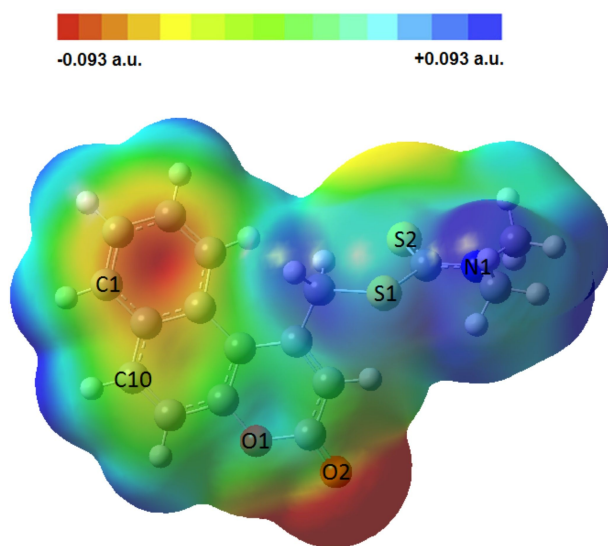


Fig. 6. The total electron density mapped with electrostatic potential surface of (3-Oxo-3H-benzo[f]chromen-1-yl) methyl N,N-dimethylcarbamodithioate compound.

As can be seen from Fig. 5, for the HOMOs, the electrons are delocalized on the sulfur atoms. For the LUMOs, the electrons are mainly delocalized on the 3-oxo-3H-chromen ring. The energy separation between the HOMO and LUMO is 3.972 eV. Also chemical hardness and stability can be calculated from the HOMO-LUMO gap and have been found to be 1.986 eV and 0.252 eV $^{-1}$, respectively [64].

3.7. Molecular electrostatic potential analysis

Molecular electrostatic potential (MEP) is related to ED and is a very useful tool for identifying the sites for electrophilic and nucleophilic reactions as well as hydrogen bonding interactions [65, 66].

In majority of MEP analyses, the maximum negative region which is the preferred site for electrophilic attack is shown in red color, the maximum positive region which is the preferred site for nucleophilic attack is shown in blue color. The MEP displays molecular size, shape as well as positive, negative and neutral electrostatic potential regions in terms of color grading and is very useful in investigating a molecular structure with its physiochemical property relationship [67]. In this study, 3D plot of MEP of the title compound is shown in Fig. 6.

As can be seen from Fig. 6, the negative regions in the molecule were found around the keto group (O2 atom) and inside the benzene ring. The negative $V(r)$ values are -0.093 a.u. for O2 atom which is the most negative region and -0.043 a.u. for the inside region of benzene ring. Therefore, we can predict that an electrophile preferably can attack the title compound at the O2 position.

Meanwhile, looking at the map in Fig. 6, a possible site for nucleophilic processes is predicted on the hydrogens of dimethylamino fragment with a value of $+0.057$ a.u. The MEP results of the title compound are in agreement with the literature [67, 68]. According to these calculated results, the MEP map shows that the most negative potential site is on keto group and the most positive potential sites are around the hydrogen atoms.

3.8. Thermodynamic properties

On the basis of B3LYP/6-311++G(d,p) vibrational analysis and statistical thermodynamics, the standard thermodynamic functions: entropy (S_m^0), heat capacity ($C_{p,m}^0$) and enthalpy (H_m^0) were obtained and listed in Table 5.

The scale factor for frequencies, which has been used for an accurate prediction of the thermodynamic functions, is 0.96 . Table 5 shows that

Table 5. Thermodynamic properties at different temperatures at B3LYP/6-311++G(d,p) level.

T [K]	H_m^0 [kcal·mol ⁻¹]	$C_{p,m}^0$ [cal·mol ⁻¹ ·K ⁻¹]	S_m^0 [cal·mol ⁻¹ ·K ⁻¹]
200	7.173	55.754	128.531
250	10.507	67.569	142.683
298.15	14.302	78.847	155.889
300	14.459	79.273	156.398
350	19.013	90.477	169.783
400	24.133	100.885	182.816
450	29.775	110.354	195.488
500	35.888	118.864	207.775
550	42.423	126.474	219.662
600	49.334	133.274	231.133

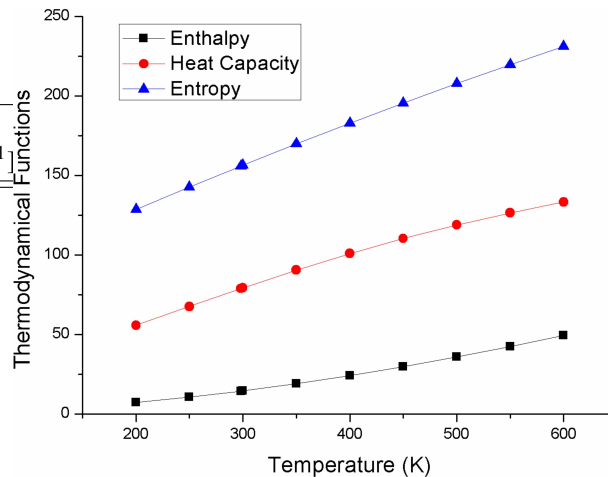


Fig. 7. Correlation plots of thermodynamic properties and temperatures.

the S_m^0 , $C_{p,m}^0$ and H_m^0 increase with temperature from 200.00 K to 600.00 K, because the intensities of the molecular vibrations increase with the increasing temperature.

The correlations between these thermodynamic properties and temperature T are shown in Fig. 7. The correlation equations are as follows:

$$C_{p,m}^0 = -1.85521 + 0.31619T - 1.49867 \times 10^{-4}T^2; \quad (R^2 = 0.99985) \quad (2)$$

$$S_m^0 = 68.25583 + 0.31622T - 7.4506 \times 10^{-5}T^2; \quad (R^2 = 1) \quad (3)$$

$$H_m^0 = -1.77879 + 0.02345T - 1.03268 \times 10^{-4}T^2; \quad (R^2 = 0.99994) \quad (4)$$

These equations will be helpful for the further studies of the title compound.

4. Conclusions

The geometric parameters and vibrational frequencies of 3-Oxo-3H-benzo[f]chromen-1-yl) methyl N,N-dimethylcarbamo-dithioate have been calculated using HF and DFT (B3LYP and B3PW91) methods with 6-311++G(d,p) basis sets. The comparison between the calculated results and

the X-ray experimental data shows that B3LYP method is better than HF and B3PW91 methods in evaluating bond lengths, angles, dihedral angles and vibrational frequencies, in which the experimental and theoretical results support each other [24]. The energy gap between the HOMO and LUMO is very large and this energy separation gives important information about the title compound. The NBO analysis revealed that the $\pi^* \rightarrow \pi^*$ interactions give the strongest stabilization to the system. On the other hand, it was found that, in gas-phase, the atomic charge values are larger than those in solution-phase and atomic charge values decrease with increasing polarity of the solvent. The correlations between the statistical thermodynamic properties (enthalpy, entropy, heat capacity) and temperatures were also studied. Our calculations are in progress and we hope that the present paper will be useful in designing and synthesis of new materials.

References

- [1] EVANS B.E., RITTLE K.E., BOCK M.G., DIPARDO R.M., FREIDINGER R.M., WHITTER W.L., LUNDELL G.F., VEBER D.F., ANDERSON P.S., CHANG R.S.L., LOTTI V.J., CERINO D.J., CHEN T.B., KLING P.J., KUNKEL K.A., SPRINGER J.P., HIRSHFIELD J., *J. Med. Chem.*, 31 (1988), 2235.
- [2] *Enraf-Nonius CAD-4 Express '88 Software*, Enraf-Nonius: Delft, Holland, 1988.

- [3] HENRIETTE G., LORRAINE L., BETTINA H., CLEMENCE D., KELLY D., IRENEJ K., *Mol. Cancer Ther.*, 3 (2004), 1375.
- [4] LAURIN P., FERROUD D., KLICH M., DUPUIS-HAMELIN C., MAUVAIS P., LASSAIGNE P., BONNEFOY A., MUSICKI B., *Bioorg. Med. Chem. Lett.*, 9 (1999), 2079.
- [5] FYLAKTAKIDOU K.C., HADJIPAVLOU-LITINA D.J., LITINAS K.E., NICOLAIDES D.N., *Curr. Pharm. Des.*, 10 (2004), 3813(30).
- [6] KWANGWOO C., SONG-KYU P., MOOK K.H., YONGSEOK C., MYUNG-HWA K., CHUN-HO P., BO-YOUNG J., GYU C.T., HYUN-MOO C., HEE-YOON L., HEE H.S., SOOK K.M., KY-YOUB N., GY-OOHHEE H., *Bioorg. Med. Chem.*, 16 (2008), 530.
- [7] SHARMA P.N., SHOEB A., KAPIL R.S., POPLI S.P., *Indian J. Chem. B*, 19 (1980), 938.
- [8] SHARMA P.N., SHOEB A., KAPIL R.S., POPLI S.P., *Indian J. Chem. B*, 17 (1979), 299.
- [9] NARESHKUMAR J., JIAYI X., RAMESH M.K., FUYONG D., GUO J.Z., EMMANUEL P., *J. Med. Chem.*, 52 (2009), 7544.
- [10] TRAYKOVA M., KOSTOVA I., *Int. J. Pharm.*, 1 (2005), 29.
- [11] DOSHI J.M., TIAN D., XING C., *J. Med. Chem.*, 49 (2006), 7731.
- [12] ALIAA M.K., MANAL M.K., EMAN K ABD EL-ALL, HEBA A.H. ELSHEMY, *Int. J. Pharm. Res. Develop.*, 4 (2012), 310.
- [13] NORTH A.C.T., PHILIPS D.C., MATHEWS F.S., *Acta Cryst. A*, 24 (1968), 351,
- [14] KAMDAR N.R., HAVELIWALA D.D., MISTRY P.T., PATEL S.K., *Medic. Chem. Res.*, 20 (2011), 854.
- [15] SHARMA P.N., SHOEB A., KAPIL R.S., POPLI S.P., *Phytochemistry*, 20 (1981), 335.
- [16] ELHAFEZ O.M.A., EL KHRISY E.D., BADRIA F., FATHY A.D., *Arch. Pharm. Res.*, 26 (2003), 686.
- [17] BHAT M.A., SIDDIQUI N., KHAN S.A., *Acta Pol. Pharm.*, 65 (2008), 235.
- [18] JONES G., JACKSON W.R., CHOI C., BERGMARK W.R., *J. Phys. Chem.*, 89 (1985), 294.
- [19] TRENOR S.R., SHULTZ A.R., LOVE B.J., LONG T.E., *Chem. Rev.*, 104 (2004), 3059.
- [20] HUNG T.T., LU Y.J., LIAO W.Y., HUANG C.L., *IEEE Trans. Magn.*, 43 (2007), 867.
- [21] KUMAR K.M., KOUR D., KAPOOR K., MAHABALESHWARAIAH N.M., KOTRESH O., GUPTA V. K., KANT R., *Acta Cryst. E*, 68 (2012), o878.
- [22] EL-BAYOUKI K.A., ALY M.M., MOHAMED Y.A., BASYOUNI W.M., ABBAS S.Y., *WJ Chem.*, 4 (2009), 161.
- [23] THOMAS N.A.N.C.Y., ZACHARIAH S.M., *Asian J. Pharm. Clin. Res.*, 6 (2013), 11.
- [24] MAHABALESHWARAIAH N.M., RAVI H.R., VINDUVAHINI M., SREEPAD H.R., KOTRESH O., *Acta Cryst. E*, 68 (2012), o3001.
- [25] FRISCH M.J., TRUCKS G.W., SCHLEGEL H.B., SCUSERIA G.E., ROBB M.A., CHEESEMAN J.R., SCALMANI G., BARONE V., MENNUCCI B., PETERSON G.A., NAKATSUJI H., CARICATO M., LI X., HRATCHIAN H.P., IZMAYLOV A.F., BLOINO J., ZHENG G., SONNENBERG J.L., HADA M., EHARA M., TOYOTA K., FUKUDA R., HASEGAWA J., ISHIDA M., NAKAJIMA T., HONDA Y., KITAO O., NAKAI H., VREVEN T., MONTGOMERY JR. J.A., PERALTA J.E., OGLIARO F., BEARPARK M., HEYD J.J., BROTHERS E., KUDIN K.N., STAROVEROV V.N., KOBAYASHI R., NORMAND J., RAGHAVACHARI K., RENDELL A., BURANT J.C., IYENGAR S.S., TOMASI J., COSSI M., REGA N., MILLAM J.M., KLENE M., KNOX J.E., CROSS J.B., BAKKEN V., ADAMO C., JARAMILLO J., GOMPERS R., STRATMANN R.E., YAZYEV O., AUSTIN A.J., CAMMI R., POMELLI C., OCHTERSKI J.W., MARTIN R.L., MOROKUMA K., ZAKRZEWSKI V.G., VOTH G.A., SALVADOR P., DANNENBERG J.J., DAPPRICH S., DANIELS A.D., FARKAS O., FORESMAN J.B., ORTIZ J.V., CIOSLOWSKI J., FOX D.J., *Gaussian 09, Revision C.01*, Gaussian, Inc.: Wallingford, CT, 2009.
- [26] DENNINGTON R., KEITH T., MILLAM J., *GaussView, Version 5*, Semichem Inc.: Shawnee Mission, KS, 2009.
- [27] ZHURKO G.A., ChemCraft, version 1.6 (build 304), 2009. <http://www.chemcraftprog.com/>.
- [28] TANAK H., AGAR A.A., BÜYÜKGÜNGÖR O., *Spectrochim. Acta A*, 87 (2012), 15.
- [29] SUNDARAGANESAN N., KALAICHELVAN S., MEGANATHAN C., JOSHUA B.D., CORNARD J., *Spectrochim. Acta A*, 71 (2008), 898.
- [30] AHMED M.K., HENRY B.R., *J. Phys. Chem.*, 90 (1986), 1737.
- [31] RAMALINGAM S., PERIANDY S., GOVINDARAJAN M., MOHAN S., *Spectrochim. Acta A*, 75 (2010), 1308.
- [32] SHELDRIK G.M., *Acta Cryst.*, A 64 (2008), 112.
- [33] BABU P.D., PERIANDY S., MOHAN S., RAMALINGAM S., JAYAPRAKASH B.G., *Spectrochim. Acta A*, 78 (2011), 168.
- [34] SUNDARAGANESAN N., ILAKIAMANI S., SALEEM H., WOJICIECHOWSKI P.M., MICHALSKA D., *Spectrochim. Acta A*, 61 (2005), 2995.
- [35] KRISHNAKUMAR V., JOHN XAVIER R., *Indian J. Pure Appl. Phys.*, 41 (2003), 597.
- [36] KRISHNAKUMAR V., PRABAVATHI N., *Spectrochim. Acta A*, 71 (2008), 449.
- [37] ALTUN A., GOLCUK K., KUMRU M., *J. Mol. Struct.*, 637 (2003), 155.
- [38] SINGH S.J., PANDEY S.M., *Indian J. Pure Appl. Phys.*, 12 (1974), 300.
- [39] SINGH R.N., PRASAD S.C., *Spectrochim. Acta A*, 34 (1978), 39.
- [40] SILVERSTEIN M., BASSLER G.C., MORRIL C., *Spectroscopic Identification of Organic Compounds*, 5th Ed., John Wiley & Sons Inc., Singapore, 1991.

- [41] ALTUN A., GOLCUK K., KUMRU M., *J. Mol. Struct.*, 625 (2003), 17.
- [42] DURIG J.R., BERGANA M.M., PHAN H.V., *J. Raman Spectrosc.*, 22 (1991), 141.
- [43] LITVINOV G., *Proceedings of the 13th International Conference on Raman Spectroscopy*, Würzburg, Germany, 1992.
- [44] GOVINDARAJAN M., GANASAN K., PERIANDY S., MOHAN S., *Spectrochim. Acta A*, 76 (2010), 12.
- [45] SILVERSTEIN R.M., BASSELER G.C., MORILL C., *Spectroscopic Identification of Organic Compounds*, Wiley, New York, 1981.
- [46] KARAKURT T., DINCER M., ÇUKUROVALI A., YILMAZ I., *J. Mol. Struct.*, 991 (2011), 186.
- [47] TECKLENBURG M.M.J., KOSNAK D.J., BHATNAGAR A., MOHANTY D.K., *J. Raman Spectr.*, 28 (1997), 755.
- [48] PAJAZK J., ROSPENK M., RAMAEKERS R., MAES G., GŁOWIAK T., SOBCZYK L., *Chem. Phys.*, 278 (2002), 89.
- [49] ARIVAZHAGAN M., KRISHNAKUMAR V., JOHN-AVIER R., ILANGO V., BALACHANDRAN K., *Spectrochim. Acta A*, 72 (2009), 941.
- [50] VARASANYI G., *Vibrational Spectra of Benzene Derivatives*, Academic Press, New York, 1969.
- [51] SILVERSTEIN R.M., WEBSTOR F.X., *Spectrometric Identification of Organic Compounds*, 6th Ed., John Wiley & Sons, New York, 1998.
- [52] COLTHUP N.B., DALY L.H., WIBERLY S.E., *Introduction to Infrared and Raman Spectroscopy*, 3rd Ed., Academic Press, Boston, MA, 1990.
- [53] SOCRATES G., *Infrared Characteristic Group Frequencies*, John Wiley and Sons, New York, 1980.
- [54] JAMES C., AMAL RAJ A., REGHUNATHAN R., HUBERT JOE I., JAYAKUMAR V.S., *J. Raman Spectr.*, 37 (2006), 1381.
- [55] LIU J.N., CHEN Z.R., YUAN S.F., *J. Zhejiang Univ. Sci. B*, 6 (2005), 584.
- [56] MUTHU S., PRASATH M., *Spectrochim. Acta A*, 115 (2013), 789.
- [57] SCHWENKE D.W., TRUHLAR D.G., *J. Chem. Phys.*, 82 (1985), 2418.
- [58] GUTOWSKI M., CHALASINSKI G., *J. Chem. Phys.*, 98 (1993), 4728.
- [59] TANAK H., AGAR A.A., BÜYÜKGÜNGÖR O., *Spectrochim. Acta A*, 118 (2014), 672.
- [60] MULLIKEN R.S., *J. Chem. Phys.*, 23 (1955), 1833.
- [61] JIAN F.F., ZHAO P.S., BAI Z.S., ZHANG L., *Struct. Chem.*, 16 (2005), 635.
- [62] FLEMING I., *Frontier Orbitals and Organic Chemical Reactions*, Wiley, London, 1976.
- [63] OBOT I.B., JOHNSON A.S., *Elixir Comp. Chem.*, 43 (2012), 6658.
- [64] PIR H., GÜNAY N., AVCI D., TAMER Ö., TARCAN E., ATALAY Y., *Arab. J. Sci. Eng.*, 39 (2014), 5799.
- [65] SCROCCO E., TOMASI J., *Adv. Quantum Chem.*, 11 (1979), 115.
- [66] LUQUE F.J., LOPEZ J.M., OROZCO M., *Theor. Chem. Acc.*, 103 (2000), 343.
- [67] TANAK H., TOY M., *J. Mol. Struct.*, 1068 (2014), 189.
- [68] EVECEN M., TANAK H., *Mater. Sci.-Poland*, 34 (2016), 886.

Received 2016-12-27
Accepted 2017-07-06